A Model of Nonlinear Wave Propagation in Horns*

KEITH R. HOLLAND, *AES Member,* **AND CHRISTOPHER L. MORFEY**

Institute of Sound and Vibration Research, University of Southampton, Southampton SO17 1BJ, UK

A model of the propagation of sound at finite levels within acoustic horns is proposed. The model is based on finite exponential elements, within which the sound field is expressible in closed analytic form. The linearly predicted sound field is corrected for nonlinear distortion at the end of each element. In order to model the dispersive standing-wave field present in the flare of many practical horn designs, the model predicts the input waveform required at the throat of a horn to give a desired waveform as output at the mouth. Comparisons between measurements of the harmonic distortion produced by loudspeaker horns and the model predictions are presented. It is concluded that the model can predict the degree of nonlinear waveform distortion associated with the propagation of large-amplitude waves in loudspeaker horns.

0 INTRODUCTION

The high electroacoustic efficiency of horn–compression driver loudspeaker systems leads to their use for the production of high sound pressure levels. This is important when horns are used in public address systems, where propagation over large distances may be required, and is the main reason for their widespread use in this application. In order to produce high levels in the far field, very high acoustic pressures and particle velocities must be present at the small throat of a horn, and particularly in the compression driver. A typical high-quality compression driver can produce sound pressure levels of over 140 dB in a plane-wave tube for an input of 1 W of electrical power. The same driver may have a thermally limited maximum power handling of 100 W, leading to sound pressure levels in excess of 160 dB at the throat of a horn to which it is attached. When a typical 10:1 or 20:1 compression ratio for the driver is considered, sound pressure levels of 170 to 180 dB are possible at the diaphragm.

The sound field within acoustic horns can be modeled, to a first approximation, using Webster's horn equation [1]. An important assumption inherent in the derivation of this equation is that the acoustic pressure and the particle velocity have infinitesimal amplitude. This enables the nonlinear terms that result from consideration of the thermodynamics of sound propagation to be neglected, resulting in a "linearized" form of the equation, which can be solved analytically. For the study of sound fields where the acoustic pressures are very small fractions of the static pressure, and the particle velocities very small fractions of the speed of sound, this assumption is a valid one, and the resultant linear equations are sufficiently accurate. It is clear from these levels that linear acoustic modeling of the horn and the driver is not likely to be valid at high drive levels.

Of the many sources of system nonlinearity possible at these levels, three are expected to be predominant. One involves the electromechanical limitations of the driver, including thermal power compression effects, magnet and gap problems, and so on. The second source of nonlinearity involves the volumetric changes in the cavity between the diaphragm and the phase plug, and the third involves nonlinear propagation within the horn and the driver, leading to the possibility of the production of shock waves. The first nonlinear mechanism is common to all electromagnetic loudspeakers, and a considerable amount of research has been devoted to both the modeling and the correction of this source of nonlinearity, references [2]–[4] being notable among the more recent publications.[1] The second source of nonlinearity is reasonably straightforward to predict and has been

* Manuscript received 1995 April 10; revised 1995 November 1 and 1996 April 29.

[1] The following papers have been published since submission of the original manuscript: W. Klippel, "Nonlinear Wave Propagation in Horns and Ducts," *J. Acoust. Soc. Am.*, vol. 98, no. 1 (1995); H. Schurer, A. P. Berkhoff, C. H. Slump, and D. E. Herrmann, "Modeling and Compensation of Nonlinear Distortion in Horn Loudspeakers," *J. Audio Eng. Soc. (Engineering Reports)*, vol. 43, pp. 592–598 (1995 July/Aug.).

reported in classic textbooks on acoustics [5], [6]. The third mechanism has been little researched to date, and this paper is concerned with the study of this source of nonlinearity. Earlier stages in the development of this work have been reported in [7], [8].

0.1 Glossary of Terms

Area profile Graph of the cross-sectional area of a horn flare as a function of axial distance along the horn; may also refer to the area of curved wavefront surfaces within a horn flare

Driver Electrodynamic transducer (usually moving coil) for generating acoustic power at the throat of a horn

Flare rate Rate of expansion of cross-sectional or wavefront area with increasing distance along a horn

Mouth End of horn having the largest cross-sectional area, from which sound is radiated into the far field

Throat End of horn having the smallest cross-sectional area, to which driver is attached

0.2 Symbols

c_0 = ambient speed of sound, m/s
f = frequency, Hz
k = acoustic free-field wavenumber, m^{-1}
l = model element length, m
m = flare rate, m^{-1}
n = number of elements
P_0 = ambient atmospheric pressure, N/m^2
p = acoustic pressure, N/m^2
S = area, m^2
T = time advance, s
t = time in sample intervals
u = acoustic particle velocity, m/s
x = axial distance, m
Z = nondimensional acoustic impedance, normalized to $\rho_0 c_0$
α = propagation coefficient, m^{-1}
γ = ratio of specific heats
ρ_0 = ambient density of propagating medium, kg/m^3
ω = radial frequency
$\hat{}$ = complex quantity

1 DESCRIPTION AND IMPLEMENTATION OF THE FINITE-AMPLITUDE MODEL

If it could be assumed that the sound field within horns, and that radiated to the far field, consisted of a single progressive wave from the throat out to infinity, the calculation of the sound field for finite amplitudes, to reasonable accuracy, would not be too difficult. However, a finite-length horn produces, to a greater or lesser extent, reflections from the mouth termination and from discontinuities within the horn flare. Sound propagation within horns is also often dispersive in nature. These complications prevent the prediction of the propagation of finite-amplitude waves in such horns using standard progressive plane-wave nonlinear distortion theory. When dealing with infinitesimal-amplitude (linear) waves, it is possible to predict directly the response at one end of a horn due to any input applied at the other, as the presence of a reflected wave does not affect the propagation of an incident wave. Such linear superposition does not apply when dealing with waves of finite amplitude. In this case the nonlinear transmission behavior of the horn cannot be obtained by modeling the nonlinear distortion of the forward and backward waves separately and then recombining them, because the forward and backward waves will interact in a complicated manner. It is therefore necessary, under these conditions, to assume that the mouth termination can be characterized by a linear radiation impedance (which is a reasonable approximation if the mouth is of sufficient size that the sound pressure level is below about 140 dB at the mouth) and to model the sound field "backward" to the input. Pla and Reethof [9] developed a model of the propagation of finite-amplitude waves in horns which included boundary-layer effects, and, because reflections were neglected, they were able to model "forward" from input to output. The model described hereafter attempts to include reflections and thus predicts the input necessary at the throat of a horn to achieve a desired output at the mouth.

In order to model horns with arbitrary area profiles using Webster's equation, it is desirable to split the horn into short exponentially shaped elements, within which the linear standing-wave solution is expressible in closed analytical form. This splitting into elements allows predictions of nonlinear behavior to be implemented in a seminumerical manner, with the linearly predicted field corrected for finite-amplitude distortion over a short distance at the end of each element. This approach involves the calculation of the linear propagation in the frequency domain, and of the nonlinear distortion in the time domain, transformation from one domain to the other being achieved using Fourier transforms.

The symbols used in the following description of the model refer to the flow diagram shown in Fig. 1.

1.1 Linear Propagation

Webster's horn equation, which can be written

$$\frac{1}{c_0^2}\frac{\partial^2 \hat{p}}{\partial t^2} - \frac{\partial^2 \hat{p}}{\partial x^2} - \left\{\frac{1}{S}\frac{dS}{dx}\right\}\frac{\partial \hat{p}}{\partial x} = 0 \qquad (1)$$

where $\hat{p} = \hat{p}(x, t)$ is the acoustic pressure and $S = S(x)$ is the cross-sectional area of the horn, describes the quasi-one-dimensional sound field in a duct with a cross-sectional area that varies along its length. $S(x)$, here referred to as the area profile of a horn, can refer to the area of curved wavefront surfaces within the horn [10]. The multiplying factor in the rightmost term in Eq. (1) represents the ratio of the rate of change of the area with distance to the area and is termed the flare rate $m(x)$ of the horn. A simple solution of Eq. (1) results from the substitution of an exponential area profile, as the flare rate is then constant along the length of the horn. A horn element possessing an exponential area profile can then

1996 July/August

be defined as $S(x) = S(0)e^{mx}$, where $S(0)$ is the area of the throat and m the flare rate of the horn element.

Assuming harmonic time dependence, the solution of Eq. (1) for an exponential horn element can be written

$$\hat{p} = \hat{p}_A e^{\hat{\alpha}+x} + \hat{p}_B e^{\hat{\alpha}-x} \quad (2)$$

where the propagation coefficients $\hat{\alpha}$ are

$$\hat{\alpha} = \frac{-m \pm \sqrt{m^2 - 4k^2}}{2} \quad (3)$$

p_A and p_B represent the complex amplitudes of the forward and backward wave components, respectively, k is the free-field wavenumber ($= \omega/c_0$), and m is the flare rate of the horn.

The linear propagation of an arbitrary waveform along a horn element can best be modeled in the frequency domain. Thus the desired starting (horn output) waveform $p_0(t)$ is transformed into the frequency domain via a Fourier transform. Given the resultant complex pressure spectrum $\hat{p}_0(f)$ at the mouth of the element, the flare rate and length of the element, and the normalized acoustic impedance at the mouth $\hat{Z}_0(f)$, the complex amplitudes of the forward and backward pressure wave components at the throat of the element, $\hat{p}_A(f)$ and $\hat{p}_B(f)$, respec-

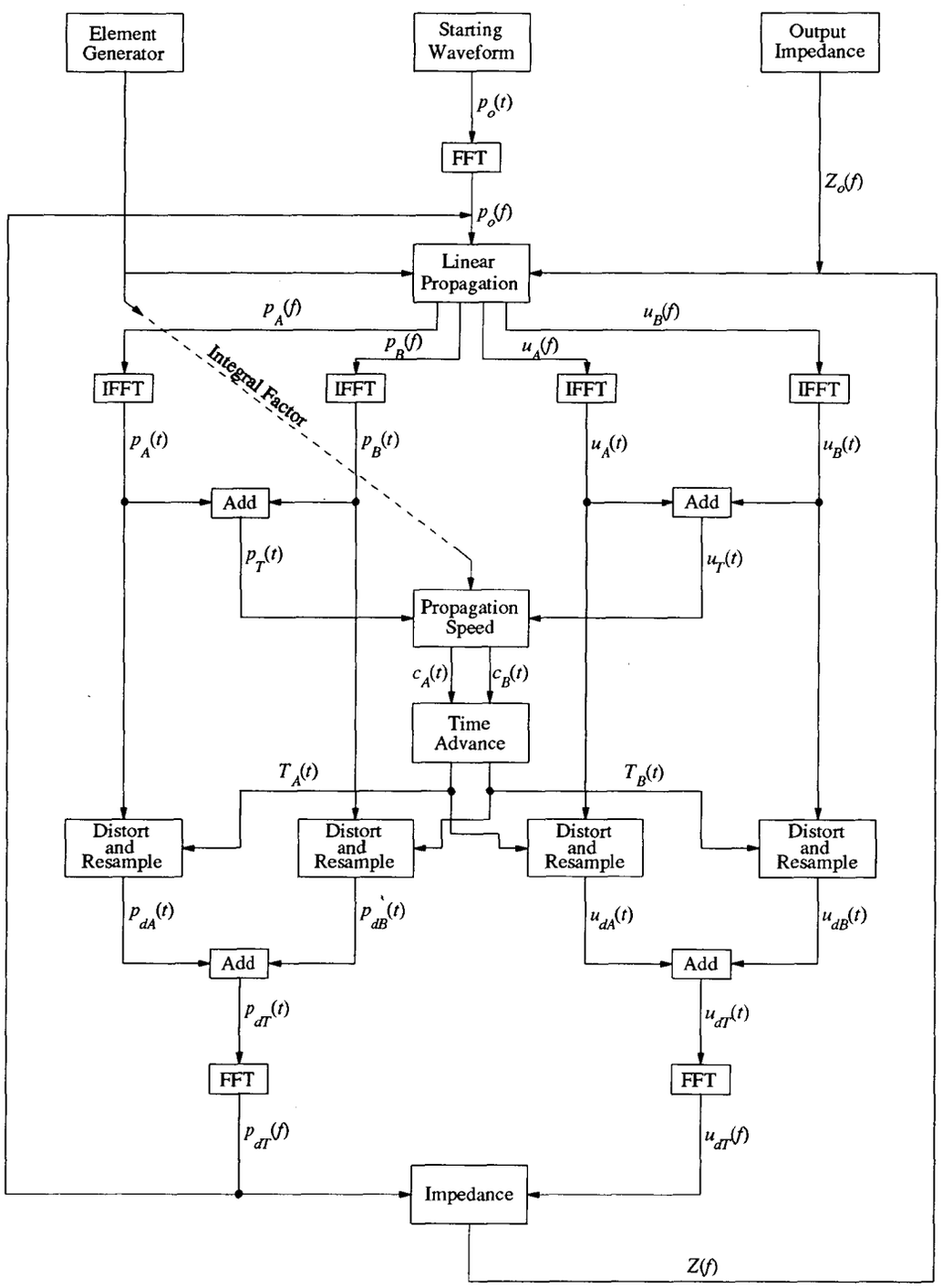

Fig. 1. Flowchart for finite-amplitude horn model.

tively, can be calculated from the solutions of Eq. (1):

$$\hat{p}_A(f) = -ik\hat{p}_0(f)\left\{\frac{1 - i\hat{\alpha}^-\hat{Z}_0(f)/k}{(\hat{\alpha}^+ - \hat{\alpha}^-)\hat{Z}_0(f)e^{\hat{\alpha}^+ l}}\right\}$$

and (4)

$$\hat{p}_B(f) = \frac{\hat{p}_0(f) - \hat{p}_A(f)e^{\hat{\alpha}^+ l}}{e^{\hat{\alpha}^- l}}$$

where l is the length of the element. The complex amplitudes of the forward and backward particle velocities at the throat, $\hat{u}_A(f)$ and $\hat{u}_B(f)$, respectively, are then

$$\hat{u}_A(f) = i\left\{\frac{\hat{\alpha}^+ \hat{p_A}(f)}{\rho_0 c_0 k}\right\}$$

and (5)

$$\hat{u}_B(f) = i\left\{\frac{\hat{\alpha}^- \hat{p}_B(f)}{\rho_0 c_0 k}\right\}.$$

These separate pressures and particle velocities are then each transformed into the time domain via inverse Fourier transforms. A full discussion of the linear part of this model can be found in [10].

1.2 Nonlinear Waveform Distortion

The speed of propagation of a sound wave at a point in the horn element is dependent on the local pressure and particle velocity at that point. At finite amplitudes this causes a waveform to distort in shape as it propagates. In a free progressive wave this results in the positive half-cycle of the waveform propagating faster than the negative half-cycle, giving rise to a steepening of sinusoids and eventual shock formation. Because of dispersion and reflections, the characteristic impedance of a wave within an exponential element is usually complex, so the equations for the calculation of waveform steepening in free progressive waves cannot be used. Instead a more universal equation for the local propagation speed $c(t)$ is necessary,

$$c(t)^{\pm} = c_0\left\{\frac{P_0 + p_T(t)}{P_0}\right\}^{(\gamma-1)/2\gamma} \pm u_T(t) \quad \text{[m/s]} \qquad (6)$$

where c_0 is the linear assumed sound speed for the particular static pressure P_0, $p_T(t) = p_A(t) + p_B(t)$ and $u_T(t) = u_A(t) + u_B(t)$ are the instantaneous total acoustic pressure and particle velocity, respectively, γ is the ratio of the specific heats of the propagating fluid, $\pm$ refers to the calculation for forward and backward waves, respectively, and (t) refers to the position in the sampled waveforms. The first term in this expression is a result of considering the adiabatic pressure–density relationship, the ideal gas equation, and the fact that the speed of sound is proportional to the square root of the absolute temperature. The time advance $T_A(t)$ or $T_B(t)$ of a sample of a waveform compared to its linear propagation can then be calculated,

$$T(t)^{\pm} = \frac{\mp l}{c_0}\left\{\frac{c_0}{c(t)^{\pm}} - 1\right\} \quad \text{[seconds]} \qquad (7)$$

where $\mp l$ is the distance propagated. The concept of a negative propagation distance is introduced to indicate modeling backward from output to input. In order to maintain linear spacing between the waveform sample points for susequent fast Fourier transform calculations, it is necessary to resample each distorted pressure and velocity waveform by interpolating between the distorted time points. This distorting and resampling process is implemented as follows.

The values of time in seconds for each of the time-domain sample points (relative to the first time point) and the calculated forward time advances are stored in arrays $time(t)$ and $T_A(t)$, respectively, along with the forward pressure waveform $p_A(t)$. The time advance array $T_A(t)$ is then inspected to find the maximum value of time advance, which is converted (rounded up) to an integer number of sample points t_{max}, and the time array $time(t)$ is added to $T_A(t)$ so that the time advances become "distorted" values of time. Each sample point (t) in $time(t)$ is then scanned from $t' = t - t_{max}$ to $t' = t + t_{max}$ sample points until $T_A(t) > time(t')$. The distorted pressure waveform $p_{dA}(t)$ then results from shifting $t' - t$ points and interpolating between the points of the undistorted waveform $p_A(t)$. Thus,

$$p_{dA}(t) = p_A(t' - 1) + \left\{\frac{[p_A(t') - p_A(t' - 1)][time(t) - T_A(t' - 1)]}{T_A(t') - T_A(t' - 1)}\right\}. \qquad (8)$$

The use of simple, linear interpolation can be justified on the grounds that the errors generated will be proportional to, and small compared with, the distortion of the waveform, and will generally be reduced by the necessary truncation of the frequency range of interest brought about by waveform sampling. This process, shown graphically in Fig. 2, is repeated for the backward pressure waveform [with $p_B(t)$, $T_B(t)$, and $p_{dB}(t)$ in place of $p_A(t)$, $T_A(t)$, and $p_{dA}(t)$] and the two velocity waveforms. As the model cannot handle shock propagation, the time advances are checked to ensure that none of the time points overlap, indicating shock generation.

The two distorted pressure time waveforms $p_{dT}(t)$ are then added and transformed into the frequency domain for use as the starting spectrum for the next element, $\hat{p}_0(f)$. The particle velocity waveforms $u_{dT}(t)$ are also added and transformed, and the frequency-domain total distorted pressure and particle velocities are used to calculate the mouth impedance for the next element. Thus,

$$\hat{Z}(f) = \frac{\hat{p}_{dT}(f)}{\rho_0 c_0 \hat{u}_{dT}(f)}. \qquad (9)$$

When the throat of the last element is reached, the total

distorted pressure or particle velocity waveform can be considered to be that input necessary at the throat of the horn to give the original starting waveform as output at the mouth.

The model as described was programmed in BBC BASIC V/VI on an Acorn Archimedes microcomputer. All of the calculations, including the fast Fourier transform and the inverse Fourier transform routines used for the time–frequency domain transformations, are carried out using either standard precision (6-byte) or IEEE double-precision (8-byte) floating-point numbers.

2 TESTING OF MODEL

2.1 Time-Domain Sample Rate

In order to give maximum resolution in the frequency domain for periodic starting waveforms such as sinusoids, the time-domain sample rate is chosen to be an integer division of the time period of the waveform. For transient starting waveforms, a suitable sample rate for the duration and bandwidth of the transient is chosen. A problem became apparent when a large number of elements were used ($n > 20$) and the starting waveform was periodic. It is reasonable to assume that any distortion should appear only as harmonics of the waveform fundamental. However, when such a starting waveform was used, spurious frequencies were observed in the spectra after propagation through a large number of elements. This was traced to the lack of any "signal" at those frequencies, allowing the rounding errors (noise) in the computations to appear as very large numbers in the calculation of impedance at those frequencies (a small number divided by a very small number giving a large number), which after a large number of elements allowed significant values for pressure to appear. A first attempt to overcome this problem was to "pad" the starting waveform with a small delta function to give some signal at all frequencies. This resulted in gross amplification at low frequencies, below the cutoff of the horn (where large amounts of "input" are necessary at the throat to appear as small outputs on the starting waveform), making the problem worse. Finally it was decided that for periodic starting waveforms, only the harmonics would be calculated in the frequency domain, all other frequencies being held to zero. This technique appears to work well. For transient starting waveforms the problem does not occur, and frequency-domain calculations are carried out at all frequencies.

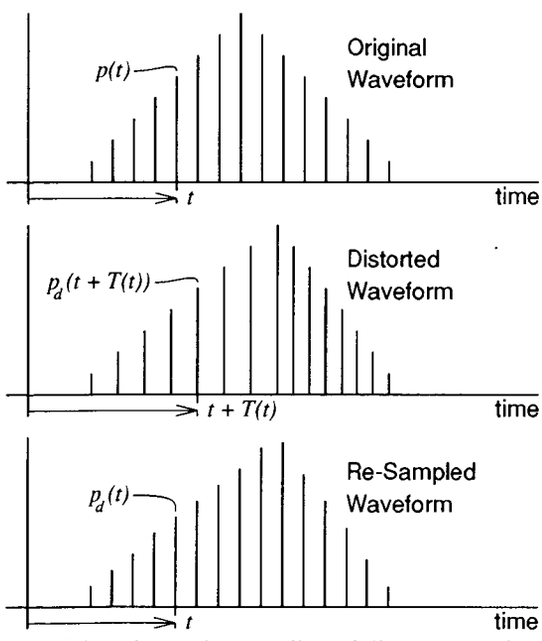

Fig. 2. Distortion and resampling of discrete waveform.

2.2 Solution Convergence

The solutions of the linearized horn equation described in Section 1.1 are accurate (within the one-parameter assumptions) for any length of element and at any frequency, provided the element area profile is exponential. When considering finite-amplitude waves, however, this is not the case, as the interactions between the forward and backward waves are likely to vary within the space of one wavelength of the highest frequency of interest. To investigate the effect of varying the number of elements on the model results, an axisymmetric horn having an exponential area profile and poor mouth termination was modeled, first using one element and then increasing the number of elements until convergence of the result was apparent. Fig. 3 shows the results of this modeling in terms of the levels of second, third, and fourth harmonics present at the throat of the horn when a sinusoidal starting waveform at a frequency of 1000 Hz and a level of 150-dB SPL is present at the mouth of the horn. The horn has a cutoff frequency of 150 Hz.

As can be seen in Fig. 3, if sufficient elements are not used, the model tends to overestimate the degree of nonlinearity compared to the result for a larger number of elements. This problem was traced to the use of the high pressure and particle velocity values that occur at the small end (throat) of each element for the speed of propagation calculations, giving the worst-case approximations to the actual degree of nonlinearity. To overcome this problem, a weighting factor (shown dashed in Fig. 1) was introduced into the calculations by assuming that, for a given forward or backward wave, the product

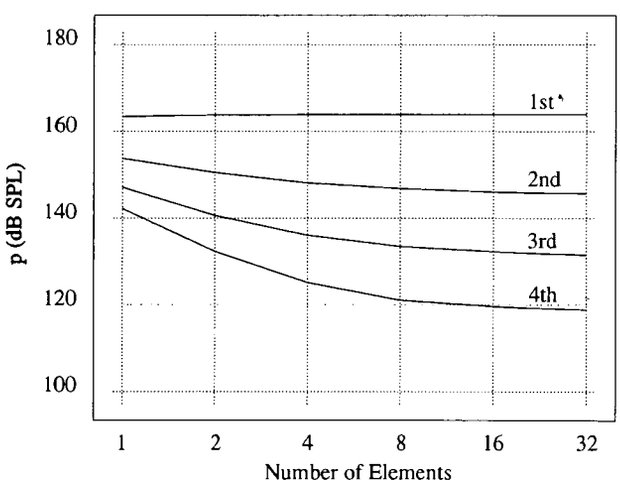

Fig. 3. Convergence of solution with increasing number of elements.

of the pressure and the square root of the area remains constant throughout an element (conservation of power flow). Because of the exponential shape of each element, the integral of this function over an element appears as a multiplying constant in terms of both pressure and particle velocity,

$$\text{factor} = \frac{1}{l}\int_0^l e^{-mx/2}\,dx = \frac{2}{ml}(1 - e^{-ml/2}) \qquad (10)$$

where l is the length and m the flare rate of the element. The only other assumption inherent in this procedure is that the distorting effect varies linearly with pressure and particle velocity over an element. This is reasonable for a short element. After this modification the convergence test was rerun, and the results are shown in Fig. 4. It can be seen that the convergence is now very much more rapid as the number of elements is increased and that more reliable results could be obtained with few elements.

2.3 Parametric Study of Model Output

The following section deals with some initial investigations into the behavior of the model when the mouth output sound pressure level and the fundamental frequency are varied. In all of these tests the starting waveform is sinusoidal, allowing the degree of nonlinearity to be estimated from harmonic distortion figures. The test results are typical for a midfrequency loudspeaker horn driven at high levels.

Fig. 5 shows the levels of the fundamental, second, third, and fourth harmonics present at the throat of the horn for a sinusoidal starting waveform (pressure at mouth) of 150-dB SPL over a range of frequencies from 100 Hz to 5 kHz. Fig. 6 shows the levels of the fundamental, second, third, and fourth harmonics present at the throat of the horn for a sinusoidal starting waveform with a frequency of 1000 Hz over a range of levels from 90 to 170-dB SPL.

3 EXPERIMENTAL VERIFICATION OF MODEL

In order to verify that the model could reliably predict the propagation nonlinearity in horns, an experiment was set up to measure the performance of a real horn for comparison with the model predictions. The initial intention was to use the model output to drive the horn via a digital-to-analog converter and then compare the waveform at the mouth of the horn with the sinusoidal starting waveform. This method would need a great deal of setting up, and the system frequency response and inherent nonlinearities prior to the horn would have to be taken into account. Even if this were done, because of the standing-wave field within the horn, the wave reflected from the mouth would be distorted, so the waveform generated by the driver would not be that of the pressure at the throat (a driver is not a perfect pressure source). Because of these complications and uncertainties, a simpler, essentially self-calibrating, method was preferred. This method involved measuring the amplitude and phase spectra of the harmonics at the mouth of the horn with a sinusoidal input to the driver, then using these measured mouth harmonics to define the starting waveform for the model. Direct comparison could then be made between measurements of the harmonics at the throat and the output from the model.

To reduce as far as possible the effects of errors in the linear part of the modeling, an axisymmetric horn having an exponential area profile and small mouth dimension was chosen for the measurements. The small mouth of this horn gives rise to a strong standing-wave field within the flare, and so provided a suitable challenge to this aspect of the modeling. The choice of a suitable means of driving the horn at very high levels was made on the basis of reliability and low inherent source nonlinearity, which ruled out the direct connection of available 1-in (25.4-mm) throat drivers. A Community M4 driver, having a 4-in (101.6-mm) throat and an output capability of over 100 acoustic watts was therefore used. Initial investigations showed that this driver produced harmonics at least 40 dB below the fundamental (1% harmonic distortion) at 150-dB SPL over the frequency range of 200 Hz to 2 kHz when driving an ideal load.

The horn was mounted in a baffle between two measurement rooms (see Fig. 7), and the driver clamped to the flange of the horn. Measurements of the sound fields were taken using a Brüel and Kjær 4135 ¼-in (6.35-mm) measurement microphone connected to a Brüel and Kjær 2032 dual-channel FFT analyzer set up to measure instantaneous power and phase spectra. A small hole, to fit the microphone, was drilled in the horn to permit measurement of the sound field at the throat. The signal source was a precision sine-wave oscillator connected to the driver via a one-third-octave filter set, a manual push-on, release-off button, and a Crown DC300 power amplifier. To guard against possible damage to the power amplifier or driver, and to ensure that unwanted sources of nonlinearity were kept to a minimum, the output from the power amplifier was monitored on the other channel of the analyzer and was observed to produce harmonic distortion at least 70 dB below the fundamental throughout the experiment. Measurements were

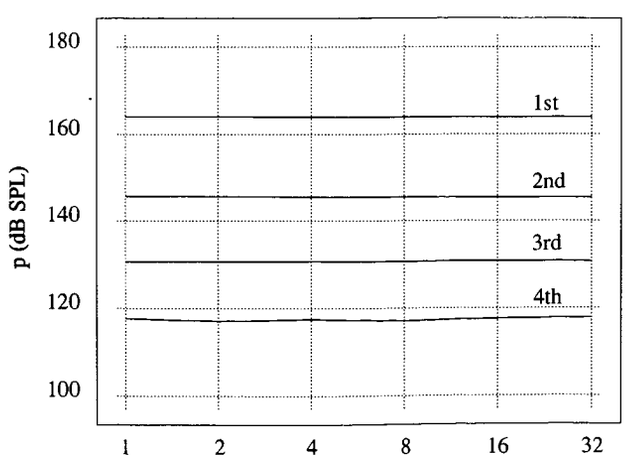

Fig. 4. Convergence of solution with integrated factor correction.